Adsorption Mechanisms of Charged, Amphiphilic Diblock Copolymers: The Role of Micellization and Surface Affinity

Ryan Toomey,[†,⊥] Jimmy Mays,[‡,§] D. Wade Holley,[‡] and Matthew Tirrell*[,†]

Department of Chemical Engineering and the Materials Research Laboratory, University of California at Santa Barbara, Santa Barbara, California 93106; Department of Chemistry, University of Tennessee, Knoxville, Tennessee 37996; and Chemical Sciences Division, Oak Ridge National Laboratory, Oak Ridge, Tennessee 37831

Received September 13, 2004; Revised Manuscript Received February 28, 2005

ABSTRACT: We have studied the adsorption of charged, amphiphilic diblock copolymers above the critical micelle concentration to develop a systematic understanding of the effects of micellization on the adsorption kinetics. Two distinct regimes are found. If the micelle−surface interaction is sufficiently weak, micelles do not adsorb and the adsorption kinetics depends only on the critical micelle concentration, that is, on the concentration of free chains in solution. When the micelle−surface interaction is attractive, micelles directly adsorb; however, the initial adsorption rate is slower than that predicted from diffusion rates alone. It is suggested that micelles must overcome a potential barrier to adsorb, the rate determined by a balance between the compressibility of the corona and the strength of the micelle−surface interaction.

Introduction

Over the past decade, the adsorption of amphiphilic diblock copolymers has attracted extensive experimental[1−8] and theoretical attention[9−12] due to the ability of these molecules to self-assemble into structured "brush" layers at surfaces. This feature has made them powerful candidates for the control and manipulation of surface properties. However, the adsorption processes of polymers can involve long relaxation times that effectively freeze in nonequilibrium states in the adsorbed layer.[13] The buildup of the layer most likely occurs by the transport of either free chains or micelles through a partially adsorbed layer, followed by a molecular rearrangement of the adsorbed species toward the thermodynamically preferred surface structure. The precise role that micelles play in this process is fundamentally important since the characteristic time scales for the brush layer assembly should be greatly affected by their presence. The degree of homogeneity achievable in a certain period could also be expected to depend significantly on whether micelles are present and active in the adsorption process.

The adsorption of block copolymers can display rather rich and varied behavior when carried out above the critical micelle concentration (cmc). If the adsorbing surface displays no affinity toward the coronal block, micelles do not adsorb and the initial adsorption rate should be set by the critical micelle concentration or the concentration of free chains in solution. Adding polymer above the critical micelle concentration only serves to create more micelles and therefore will not impact adsorption times. If the cmc is sufficiently low, adsorption may not even be observed on an experimental time frame. For instance, Dewalt et al.[14] found that block copolymers of poly(styrene-*b*-ethylene oxide) did not adsorb to polystyrene particles from aqueous solution, where PEO displays no affinity for the polystyrene particles. Only by adding tetrahydrofuran, a good solvent for the polystyrene, did they find considerable adsorption rates. This observation suggests that, in water, micelle formation effectively ties up most of the free chains and strongly hinders adsorption.

If, on the other hand, the corona of the micelle displays an affinity toward the surface, direct micelle adsorption may be possible. For instance, Hong et al.[15] found evidence that poly(styrene-*b*-2-vinylpyridine) micelles adsorb to silver substrates in toluene, and Webber et al.[16] showed that poly(2-(dimethylamino)ethyl methacrylate-*b*-methyl methacrylate) micelles adsorb directly to mica from aqueous solutions. In both cases, it was demonstrated that the equivalent homopolymer comprising the corona of each micelle also adsorbed to each respective surface, providing a rationale for micelle adsorption. However, in the case of such systems, there have been few experimental studies aimed at understanding the adsorption rate of micelles with respect to their structure. Despite an affinity of the coronal block to the surface, it is still expected that the corona must deform upon adsorption, an energetically unfavorable event.[17] As a consequence, the adsorption of micelles is expected to follow different behavior than that of individual coils, which usually show negligible resistance to adsorption and tend to adsorb more quickly than their supply rate to the surface.

A third type of adsorption behavior has also been experimentally observed, where despite evidence that micelles do not adsorb, the adsorption rate is still faster than that suggested by the free chain concentration alone. For instance, Bijsterbosch et al.[18] reported significant adsorption of poly(dimethylsiloxane-*b*-2-ethyl-2-oxazoline) to titanium dioxide despite an extremely small value for the cmc and no apparent affinity of the soluble block to the surface. Munch et al.[19,20] found that the rate of adsorption of poly(ethylene oxide-*b*-styrene) micelles to sapphire in cyclopentane depends weakly on the overall micelle concentration even though the coronal block, polystyrene, does not adsorb to the surface. An explanation of such anomalous behavior has been

[†] University of California at Santa Barbara.
[‡] University of Tennessee.
[§] Oak Ridge National Laboratory.
[⊥] Current address: Department of Chemical Engineering, University of South Florida, Tampa, FL 33620.
* Corresponding author: e-mail tirrell@engineering.ucsb.edu.

10.1021/ma048121x CCC: $30.25
Published on Web 05/19/2005

Table 1. Polymer Molecular Characteristics

sample	M_w NaPSS	M_w PtBS	M_w/M_n	% sulfonation[a]	N_{NaPSS}[b]	N_{PtBS}[b]
$NaPSS_{444}$	87 000		1.1	90	444	
$PtBS_{15}$-*b*-$NaPSS_{438}$	86 000	2400	1.05	89	438	15
$PtBS_{26}$-*b*-$NaPSS_{413}$	83 000	4100	1.03	89	413	26

[a] Sulfonation degree is calculated from the elemental analysis analysis data on sulfur. [b] Weight-average degree of polymerization.

offered by Johner and Joanny, who argue that the adsorption rate could perhaps be influenced by micelle relaxation near the interface.[10] In the early stages of adsorption, the region next to the adsorbing surface is depleted of free chains breaking the local equilibrium between free chains and micelles. If, to reestablish the local equilibrium, micelles in this zone relax and release individual chains, which themselves can adsorb, the formation of the adsorbed layer may be accelerated and governed by this relaxation rate. These relaxation rates, however, are not well-known for diblock copolymer micelles, and it is uncertain whether this phenomenon explains the above observations.

In this paper, we delineate how diblock copolymers can initially populate an empty surface. Ellipsometry is used to study the adsorption kinetics of poly(*tert*-butylstyrene-*b*-sodium styrenesulfonate) (PtBS-*b*-NaPSS) from aqueous solutions to both hydrophilic SiO_2 and hydrophobic OTS surfaces. NaPSS shows an affinity to both surfaces; however, the affinity to OTS surfaces is greater, presumably due to the strong hydrophobic interaction between the carbon−carbon polymer backbone and the hydrocarbon OTS surface.[21] The PtBS-*b*-NaPSS copolymers are highly asymmetric, with the hydrophobic poly(*tert*-butylstyrene) block only comprising 3% of the molecular weight. The solutions are characterized by extremely low critical micelle concentrations ($<10^{-3}$ mg/mL) and form so-called "hairy" micelles characterized by radii of gyration that are much larger than the constituent chains. For comparison purposes, the adsorption behavior of NaPSS homopolymer is also studied.

Materials and Methods

Materials. Diblock copolymers of PtBS and NaPSS were produced by sulfonation of a precursor diblock of PtBS and polystyrene (PS), which was prepared by anionic polymerization. The material was selectively sulfonated by the method of Valint and Block to yield approximately 90% sulfonation.[22−24] The sulfonic acid groups were neutralized using sodium methoxide to generate the final diblock copolymers. To ensure water solubility, the copolymers were made highly asymmetric with a small hydrophobic PtBS block relative to a large NaPSS block. The molecular characteristics of the polymers are shown in Table 1. NaPSS homopolymer of molecular weight 87 000 was purchased from Polysciences and used as received. Optically clear solutions were obtained by dissolving the polymer in Milli-Q water at a known concentration (100−500 ppm) and stirring for 2−4 weeks. At approximately 1 week prior to the experiment, the solutions were diluted to the desired concentration, and the appropriate amount of sodium chloride was added. At this time, the solutions were gently stirred at 90 °C for 3 days followed by 4 days at room temperature to ensure equilibrium and reproducibility of the solution. Immediately before the experiment, the solutions were filtered through a 0.45 μm polycarbonate filter.

Silicon surfaces for adsorption were prepared in the following way. (100)-oriented, double-sided polished, test grade silicon wafers (Virginia Semiconductor) were cut into pieces of appropriate size (~1 cm^2) and cleaned by a two-step process. First, they were dipped into a freshly made 70:30 (v/v) sulfuric acid/hydrogen peroxide solution for 10−15 min followed by rinsing under Milli-Q water for 3−5 min. To remove any remaining contaminants, the wafers were exposed to a UV cleaning chamber between 5 and 10 min. The UV light source was a low-pressure mercury quartz lamp. This treatment yields a hydrophilic, contaminate-free surface with a native oxide (SiO_2) layer of 14−15 Å thick, as checked by ellipsometry. Water will completely wet the treated surface. If the treatment produced a finite contact angle with water, the cleaning process was repeated. These cleaned surfaces were used within 10 min of preparation.

To prepare the hydrophobic surfaces, octadecylsilane (OTS) films were made by immersing the substrates in 10^{-3} mol/L solutions of octadecyltrichlorosilane in toluene for 1−2 h. Octadecyltrichlorosilane (Aldrich, 95%) and toluene (Sigma-Aldrich, HPLC grade, 99.8%) were commercially available and used as received. The coating solutions were used for no more than 1−2 days, after which they were discarded and new solutions made. The film-covered substrates were then removed from the solution and baked at 110 °C for 1 h to remove any excess water and drive complete hydrolysis of the OTS layer. If the OTS deposition was successful, the toluene solution will dewet the surface and bead off as the substrate is removed. Following the baking step, the substrates were sonicated in HPLC grade chloroform to remove any loose OTS.

Ellipsometry showed the final film thickness was on the order of 20−22 Å (the contour length of a single molecule is 26 Å); therefore, the surface coverage is on the order of 80%. Typical advancing angles were 110°−115° and receding angles were 100°−105°. Receding angles of less than 95° indicated a poorly formed layer, and in the rare occasions when this occurred, these substrates were discarded.

Ellipsometery Measurements. All adsorption experiments were conducted with a Beaglehole picometer ellipsometer, which uses a He−Ne laser light source (λ = 632.8 nm), has an angular resolution of 1/100, and is based on phase modulation technique of Jasperson and Schnatterley.[25] The ellipsometer directly measures the real and imaginary components of the ellipsometric ratio[26]

$$\rho = \frac{r_p}{r_s} = \tan \Psi e^{i\Delta} \tag{1}$$

where $\mathrm{Re}(\rho) = \tan \Psi \cos \Delta$ and $\mathrm{Im}(\rho) = \tan \Psi \sin \Delta$. r_p and r_s are the complex overall reflection coefficients of the p and s polarizations, respectively. The angles Ψ and Δ correspond to the ratio of attenuation of the p and s polarizations and the phase change between the p and s polarizations, respectively.

At the beginning of the experiment, either a freshly cleaned silicon substrate or an OTS/silicon substrate was inserted into a specially built cylindrical solution cell. The cell was then filled with polymer-free solution at the desired salt concentration. The angle of incidence was set at the Brewster angle (~71°) for the water/silicon interface. At this angle, $\Delta = 90°$ and $\mathrm{Im}(\rho) \leq 0.005$. If $\mathrm{Im}(\rho)$ remained constant over the next 15 min, the polymer solution was introduced through the cell inlet. The adsorbed amount Γ (mass/area) was then determined using the following analysis[27]

$$\mathrm{Im}(\rho) - \mathrm{Im}(\rho)_{\mathrm{baseline}} = \frac{2\pi}{\lambda} \frac{\sqrt{n_{\mathrm{solvent}}^2 + n_{\mathrm{substrate}}^2}}{n_{\mathrm{solvent}}} \left(\frac{dn}{dc}\right) \Gamma \tag{2}$$

where λ = 632.8 nm, $n_{solvent}$ = 1.33, $n_{substrate}$ = 3.88, and dn/dc = 0.168 mL/g. The refractive index increment dn/dc for the copolymers was measured with a standard Abbe refractometer.[28] The dn/dc values of both the NaPSS homopolymer and

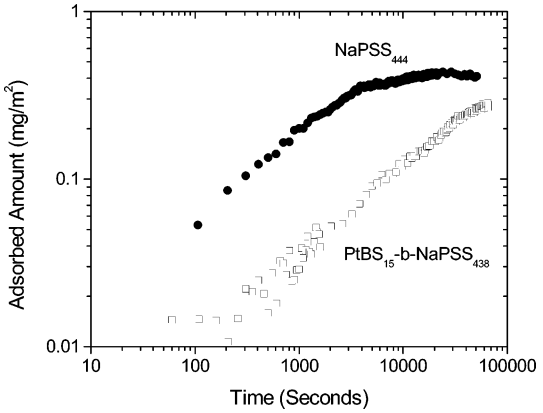

Figure 1. Comparison of the adsorption behavior of $NaPSS_{444}$ (●) and $PtBS_{15}$-*b*-$NaPSS_{438}$ (□) to a hydrophilic SiO_2 surface. Both polymers were adsorbed at a concentration of 87 ppm and 0.3 M NaCl.

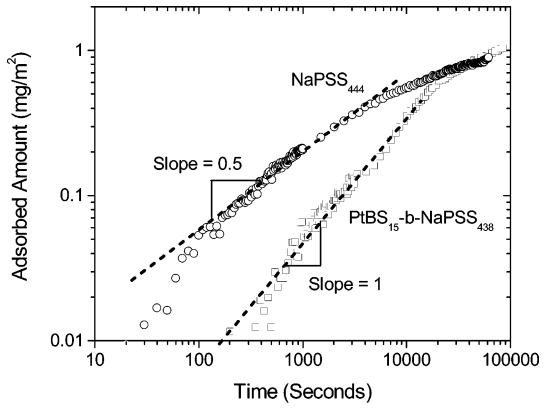

Figure 2. Log−log plot comparing the adsorption behavior of $NaPSS_{444}$ (○) and $PtBS_{15}$−$NaPSS_{438}$ (□) to a hydrophobic OTS surface. Both polymers were adsorbed at a concentration of 1 ppm and 0.3 M NaCl.

the NaPSS/PtBS diblock copolymers were approximately the same due to the relatively small size of the PtBS blocks.

Dynamic Light Scattering. Dynamic light scattering experiments were performed with a commercial goniomer and correlator purchased from Brookhaven Instruments. A He−Ne laser at a wavelength of 632 nm was used as the light source. All autocorrelation functions $g_q(t)$ were measured at 0.3 M NaCl over both a range of scattering angles (60°, 90°, 120°) and polymer concentration (100−1000 ppm). Data analysis was performed by the CONTIN Laplace transform method, which characterizes the distribution of relaxation times in the experimental time correlation window. The free particle diffusion coefficient and corresponding hydrodynamic radius of each sample exhibited very little angular dependence, and thus only the hydrodynamic radii at 90° are reported.

Results and Discussion

Figure 1 compares the adsorption of the $NaPSS_{444}$ homopolymer and the $PtBS_{15}$-*b*-$NaPSS_{438}$ copolymer from a 0.3 M NaCl solution to a hydrophilic SiO_2 surface at a concentration of 87 ppm (87 mg/L). The molecular weight of the NaPSS block in both cases is approximately the same to illustrate the effect of the insoluble PtBS block on the adsorption kinetics. Surprisingly, the adsorption rate of the homopolymer is faster than the copolymer. The homopolymer reaches a plateau value of approximately 0.4 mg/m^2 in 3 h, whereas the copolymer only reaches 0.1 mg/m^2 in the same time. Even after 10 h, the copolymer layer has only achieved $^1/_2$ the surface coverage of the homopolymer layer.

It may be somewhat unexpected that NaPSS would adsorb to SiO_2. At neutral pH, SiO_2 carries a slight negative charge that should repel like charged NaPSS chains. However, the hydrophobic nature of the NaPSS backbone combined with the high ionic strength at which adsorption was conducted must be sufficient to overcome any significant charge repulsion. Nonetheless, it is assumed that NaPSS only weakly attaches to SiO_2. This is somewhat supported by the plateau surface coverage at long times, approximately 0.43 mg/m^2, which closely corresponds to value at which the adsorbed chains begin to physically overlap. The hydrodynamic radius of $NaPSS_{444}$ at 0.3 M NaCl was determined to be 66 Å based on DLS measurements. For chains of sufficiently high molecular weight M in a good solvent, the ratio of the radius of gyration R_g to the hydrodynamic radius R_h is $R_g/R_h = 1.6$.[29] Therefore, the overlap surface coverage is predicted to be $M/\pi R_g^2 = 0.4$ mg/m^2. In the formation process of the adsorbed layer, macromolecules find and adsorb to empty sites, driven by nonelectrostatic interactions. However, because of the opposing effect of electrostatic repulsive forces between the surface and polymer segments as well as the segments themselves, it is expected that the adsorbed polymers tend to maintain a configuration close to their solution coil size.[30] As the layer reaches the condition where the neighboring chains begin to overlap, unbound polymer chains can no longer find empty space, and further adsorption is strongly quenched. On the other hand, if the monomer−surface interaction is sufficiently strong, considerable distortion of the adsorbed coil can occur, and adsorbed amounts much higher than the overlap surface coverage can result.[31]

Figure 2 shows the adsorption of the same two samples, $NaPSS_{444}$ and $PtBS_{15}$-*b*-$NaPSS_{438}$, but this time to the hydrophobic OTS surface. Again, as with the hydrophilic surface, the trend is somewhat surprising in that the homopolymer layer is formed more quickly, at least initially, than the copolymer layer. On the other hand, the surface coverage of the copolymer layer eventually surpasses the surface coverage of the homopolymer at long times. After 24 h, the homopolymer layer reaches a plateau value near 1 mg/m^2, which is a reflection of the stronger affinity between NaPSS and the hydrophobic surface. This observation is consistent with a recent study of the adsorption of NaPSS to hydrophobic interfaces.[32] The copolymer layer attains the same value of 1 mg/m^2 in 10 h and continues to grow logarithmically slowly. After 48 h, the adsorbed amount of the copolymer nears 1.4 mg/m^2.

In the start of the adsorption experiment, when the surface is still relatively bare, the upper limit for the adsorption kinetics is set by the diffusion-limited transport of the adsorbing species to the surface, as described by[10]

$$\Gamma(t) = \sqrt{\frac{4Dt}{\pi}}\, C_b \qquad (3)$$

where Γ is the adsorbed amount, D is the diffusion coefficient, and C_b is the concentration of the adsorbing species. This equation is valid only in the absence of convection and assumes that each impinging species sticks to the surface. Dynamic light scattering of $NaPSS_{444}$ homopolymer at 0.3 M NaCl yields a diffusion coefficient D of 3.4×10^{-7} cm^2/s. Superimposing the predicted initial adsorption rate from eq 3 in Figure 2

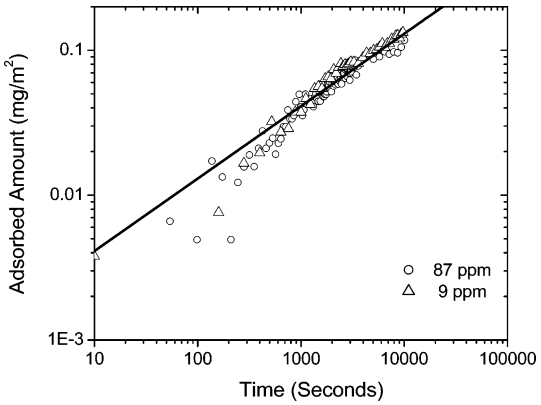

Figure 3. Adsorption of $PtBS_{15}$-*b*-$NaPSS_{438}$ at 0.3 M NaCl to a hydrophilic SiO_2 surface. The two curves show a 10-fold change in the adsorbing concentration. The solid line is fit to eq 3 showing a $t^{1/2}$ dependence, with a diffusion rate of 3.4×10^{-7} cm²/s and an effective adsorbing concentration of 0.2 ppm according to eq 3.

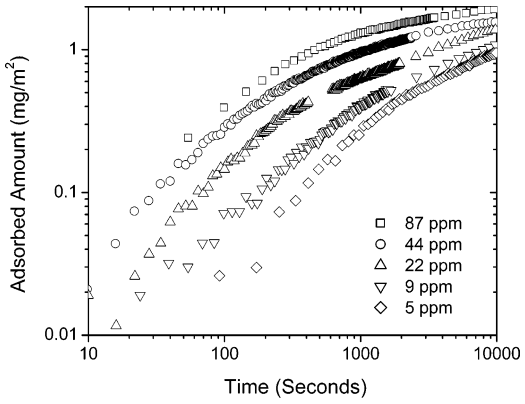

Figure 4. Adsorption of $PtBS_{15}$-*b*-$NaPSS_{438}$ to OTS at 0.3 M NaCl as a function of the overall polymer concentration.

shows that the initial adsorption kinetics of the homopolymer to the OTS surface is well described by the diffusion-limited transport mechanism with square-root-time kinetics. The copolymer, on the other hand, initially adsorbs almost 10 times more slowly than the homopolymer and shows an approximately linear time dependence, which is the characteristic signature of "reaction-limited" adsorption. Previous studies have shown that the critical micelle concentration of PtBS-*b*-NaPSS copolymers is well below 1 ppm.[33,34] Therefore, the diminished rate of diblock copolymer adsorption must be attributed to micelle formation.

At first, it may be assumed that the copolymer layer forms more slowly than the homopolymer layer due to the slower diffusion rates associated with micelles. The measured diffusion coefficient of a $PtBS_{15}$-*b*-$NaPSS_{438}$ micelle is 1×10^{-8} cm²/s, indicating that single chains diffuse 3 times as quickly as the corresponding micelles. According to eq 3, therefore, the micelles should adsorb 1.7 times more slowly than free chains. However, the difference in the diffusion rates alone is not a satisfactory explanation of the reduced adsorption rate of the micellar solution. Instead, the limiting step must somehow be related to the hindered ability of a micelle to adsorb. The next two subsections will study in detail micelle adsorption to both the hydrophilic SiO_2 and hydrophobic OTS surfaces.

Adsorption to SiO_2. Figure 3 shows the adsorption of $PtBS_{15}$-*b*-$NaPSS_{438}$ adsorbed at 9 and 87 ppm to SiO_2, an order of magnitude increase in the adsorbing concentration. Interestingly, over this range, the adsorption rate is independent of the overall polymer concentration. This observation suggests that micelles do not adsorb to SiO_2. Since both of these polymer concentrations are above the critical micelle concentration, an increase in polymer concentration only leads to the formation of more micelles, and the free chain concentration remains approximately constant. The adsorption kinetics in the first 10 000 s (~3 h) yields a square-root time dependence (as shown by the solid line). Therefore, fitting the data to eq 3 and using a diffusion coefficient of $D = 3.4 \times 10^{-7}$ cm²/s, the adsorbing concentration C_b that gives the best fit is approximately 0.2 ppm, which is in agreement with the expected critical micelle concentration.[33]

Since the adsorption of free chains locally breaks the equilibrium between free chains and micelles, micelles next to the interface may relax and release chains that may themselves adsorb. If the micelles relax more quickly than the time needed to reach a saturated layer, then the adsorption kinetics should cross over to a linear time dependence and follow a faster rate of formation than expected on the basis of the critical micelle concentration alone.[10] Furthermore, in the relaxation driven adsorption regime, there would be a rate dependence on the overall micelle concentration. Since neither of these characteristics is observed in the data, it can be concluded that micelle relaxation does not occur on a time scale fast enough to influence the adsorption rates.

Adsorption to OTS. Adsorption of the copolymer to the hydrophobic surface displays qualitatively different behavior than to the hydrophilic surface. A two-step adsorption process is clearly seen, wherein the adsorption is initially linear in time followed by a monotonically decreasing power law. Figure 4 shows the adsorption of $PtBS_{15}-PSS_{438}$ to OTS at 0.3 M NaCl over a concentration range of 5−87 ppm. Two trends emerge from the data. First, the initial rate is highly dependent on the overall concentration, which is distinct from adsorption to the hydrophilic SiO_2 surface, where micelles are excluded from adsorbing. Second, the rate of adsorption to OTS is much faster than to SiO_2. At the end of 3 h, the adsorption to OTS for the 87 ppm sample nears 2.0 mg/m², a 10-fold-increase over adsorption to SiO_2. Clearly, micelles must now be participating in the adsorption process.

To demonstrate the fact that the entire polymer population is contributing to the growth of the layer on the OTS surface, the initial rate ($d\Gamma/dt$) of the $PtBS_{15}$-*b*-$NaPSS_{438}$ copolymers is plotted against their adsorbing concentration in Figure 5, which shows a linear dependence. For comparison purposes, the initial rate of $NaPSS_{444}$ homopolymer and a $PtBS_{15}$-*b*-$NaPSS_{438}$ copolymer under the same conditions is also shown. In each case, the homopolymer initially adsorbs the fastest. Somewhat surprising is the 5-fold reduction in the initial adsorption rate of the $PtBS_{26}$-*b*-$NaPSS_{413}$ micelles in comparison to $PtBS_{15}$-*b*-$NaPSS_{438}$, where the insoluble PtBS blocks differ by almost a factor of 2. Figure 6 clarifies the adsorption behavior by showing the initial rate of each sample polymer sample at a concentration of 87 ppm vs its respective diffusion coefficient. Since the critical micelle concentration is much lower than the adsorbing concentration of 87 ppm, the diffusion coefficients of the micelles were used for the copolymer samples. It can readily be seen that the diffusion rate

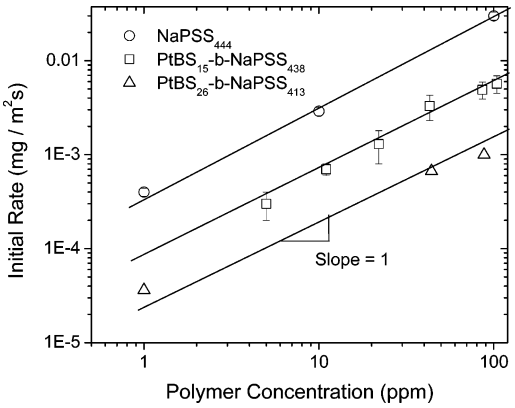

Figure 5. Initial adsorption rates of $NaPSS_{444}$ (○), $PtBS_{15}$-*b*-$NaPSS_{438}$ (□), and $PtBS_{22}$-*b*-$NaPSS_{413}$ (△) onto OTS as a function of polymer concentration at 0.3 M NaCl. The initial rate is a linear function of polymer concentration.

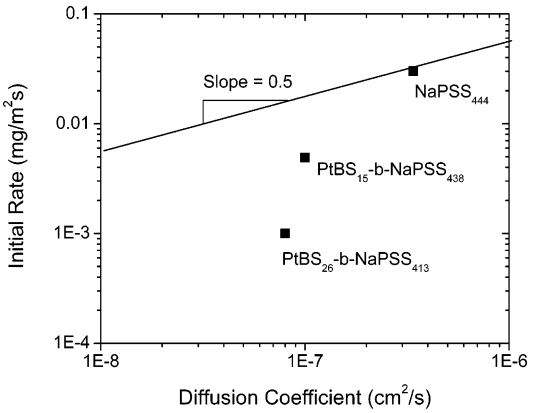

Figure 6. Log−log plot showing the initial adsorption rate of the $NaPSS_{444}$ coils, $PtBS_{15}$-*b*-$NaPSS_{438}$ micelles, and $PtBS_{26}$-*b*-$NaPSS_{413}$ micelles vs the respective diffusion coefficient. All adsorptions were conducted at 87 ppm and 0.3 M NaCl to OTS surfaces. Also plotted is a trend line that corresponds to $D^{1/2}$, which would be expected if the adsorption rate were limited by the supply rate of the adsorbing species to the surface.

alone is not a suitable predictor of the adsorption rate of the copolymer micelles. If the initial adsorption was controlled by the diffusion time for an adsorbing species to reach the surface, the initial rate should vary as the square root of the diffusion coefficient.

Because of the confinement of chains in the corona of a micelle, it is assumed that the chains in a micelle are less accessible to a surface than a free, unaggregated chain. Therefore, a constrained structure such as a micelle may be less likely to adsorb compared to a free chain. It is assumed that this free energy penalty is mostly due to compression and distortion of the corona. It has been suggested that the deformation penalty has the form[10]

$$U(d) = kTp^{3/2}\left(\frac{d}{R_{\text{corona}}}\right) \tag{4}$$

where d is the distance of the micelle from the surface, R is the radius of the corona, and p is the aggregation number. Compression of the corona with an aggregation number as low as 5 requires roughly $11kT$ of energy, which would seem to preclude the adsorption of micelles in the absence of any other driving forces. However, the hydrophobic surface may also lower the energy barrier sufficiently so that the micelles can adsorb. Particular driving forces could now stem from a strong PSS− surface interaction and a sufficiently long-ranged hydrophobic attraction between the micellar core and the surface. If the deformation penalty dominates the adsorption, then the initial rate should be expected to follow

$$\frac{d\Gamma}{dt}\Big|_0 \propto \exp(-U_{\max}/kT)C_b \tag{5}$$

On the basis of these arguments, the differences in the rates of $PtBS_{15}$-*b*-$NaPSS_{438}$ and $PtBS_{26}$-*b*-$NaPSS_{413}$ are most likely dictated by the deformation resistance of the corona. Since the aggregation number is expected to scale as $N_A^{4/5}$, the aggregation number of the $PtBS_{26}$ micelle is expected to be approximately $1\frac{1}{2}$ times the aggregation number of the $PtBS_{15}$ micelle.[10] Therefore, there may be a delicate, yet complex, balance between the deformation of the micellar corona and the number of contacts its arms can make with the surface, the balance of which determines the rate at which the micelle can overcome the potential barrier associated with adsorption and therefore the rate of the initial adsorption event. If the attractive potential cannot overcome the deformation energy, then the micelle cannot adsorb, as seen with the SiO_2 surfaces.

Effect of Cosolvents. The micelles formed by the PtBS-*b*-PSS copolymers used in this study show no signs of relaxation, or the release of free chains, in the depletion zone next to the adsorbing surface, as previously discussed. This is consistent with a previous investigation by van Stam et al., who observed that poly(*tert*-butylstyrene-*b*-sodium methacrylate) diblock copolymers with approximately the same molecular weight range did not have measurable exchange kinetics at room temperature.[35] Adding dioxane in a 1:1 molar cosolvent/polymer ratio, however, drastically enhanced the mobility of the hydrophobic core and allowed the micelles to release individual chains with time constants on the order of minutes. It is expected that micelle relaxation only accelerates the adsorption process in the early stages of layer formation, when the potential barrier due to the adsorbed layer is still not yet relevant. Since the characteristic times for $PtBS_{15}$−PSS_{438} to fully populate either the hydrophilic SiO_2 or the hydrophobic OTS surface are on the order of minutes to hours, it is anticipated that dioxane could be used to tune the initial rate of layer formation and growth.

Figure 7 shows the adsorption of $PtBS_{15}$-*b*-$NaPSS_{438}$ to the SiO_2 surface with the addition of 10 dioxane molecules per polymer chain. For comparison, the adsorption kinetics of the $NaPSS_{444}$ homopolymer is also shown. Because of the weak affinity between PSS and SiO_2, PSS_{438}−$PtBS_{15}$ micelles are excluded from the adsorption process, and the adsorption rate is governed by the free chain concentration. The effect of dioxane can be readily seen. The adsorption rate of the copolymer is enhanced by an order of magnitude over that of the copolymer solution without dioxane and approaches the rate of $NaPSS_{444}$ adsorption. After 3 h, the copolymer and the homopolymer have produced surface coverages that are almost identical. Running the experiment for longer times produces a copolymer layer that reaches $\approx$0.35 mg/m^2, slightly less than the homopolymer surface coverage at its plateau value. No evidence was seen that suggests that the copolymer/dioxane solution, with its initial enhanced adsorption rate, eventually surpasses the surface coverage of the homopolymer layer.

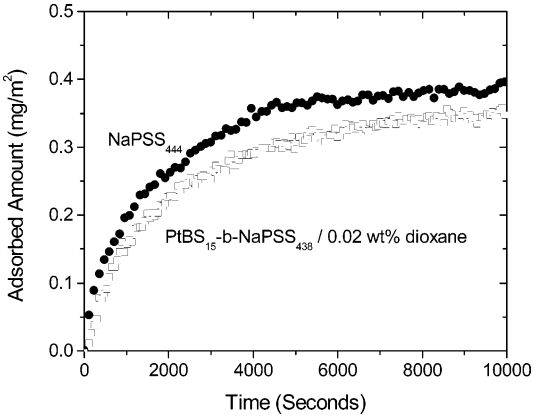

Figure 7. Adsorption of $NaPSS_{444}$ homopolymer (●) compared to the adsorption of $PtBS_{15}$-*b*-$NaPSS_{438}$ with 0.02 wt % dioxane (□) at 87 ppm and 0.3 M NaCl. Both are adsorbed to the hydrophilic SiO_2 surface.

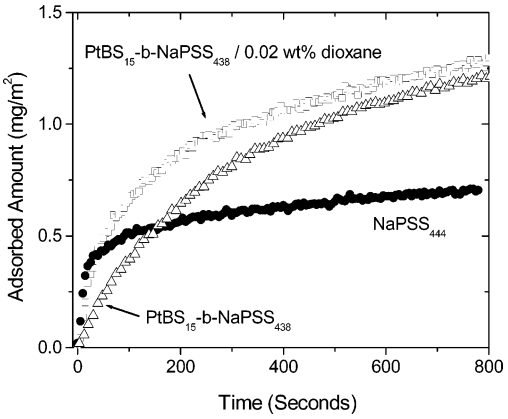

Figure 8. Adsorption of PSS_{444} homopolymer (●) compared to the adsorption of $PtBS_{15}$-*b*-$NaPSS_{438}$ with 0.02 wt % dioxane (□) at 0.3 M and $PtBS_{15}$-*b*-$NaPSS_{438}$ without dioxane (△). All are adsorbed at a concentration of 87 ppm and 0.3 M NaCl to a hydrophobic OTS surface.

Even though micelle relaxation may accelerate the initial adsorption rate of a micellar solution, when the adsorbed layer becomes dense enough, the potential barrier for the adsorption of new chains is high and passage through this barrier becomes the rate-limiting step. In this regime, it is expected that the free chain concentration next to the surface should be close to the cmc, and therefore adsorption will be independent of micelle relaxation. Because of the extremely low cmc of the current system and absence of micelle adsorption to SiO_2, it is doubtful that $PtBS_{15}$-*b*-$NaPSS_{438}$ can adsorb beyond the surface coverage of the NaPSS homopolymer on realistic time scales.

For the hydrophobic OTS surface, where it was found that direct micelle adsorption is active and contributes to rapid growth of the layer, the addition of dioxane to $PtBS_{15}$-*b*-$NaPSS_{438}$ has a smaller effect on the initial adsorption kinetics. Figure 8 shows the adsorption kinetics for the $PtBS_{15}$-*b*-$NaPSS_{438}$ with the addition of 10 dioxane molecules per each polymer chain. Also shown for comparison purposes are $PtBS_{15}$-*b*-$NaPSS_{438}$ without the addition of dioxane and $NaPSS_{444}$, all at the same adsorbing concentration. Again, as with the SiO_2 surface, the presence of dioxane cosolvent initially accelerates the initial rate of layer formation for $PtBS_{15}$-*b*-$NaPSS_{438}$. This presumably stems from the relaxation of micelles in the vicinity of the adsorbing surface due to the depletion of free chains. The released chains subsequently adsorb more quickly than the micelles themselves and accelerate the adsorption rate, although adsorption of the homopolymer remains twice as fast. Even if the micelles were able to break up immediately in the vicinity of the substrate, the adsorption rate would still be limited by the supply rate of micelles to the interface. Since micelles diffuse more slowly than the individual chains, it is thus expected that more time is always necessary for a micellar solution to initially populate a barren surface than free, unassociated chains.

Above the expected overlap surface coverage for NaPSS coils, 0.4 mg/m^2, there is a sharp decrease in the rate of formation of the homopolymer layer, followed by slow logarithmic growth until about 1 mg/m^2. The PtBS-*b*-NaPSS/dioxane mixture shows a much more rounded transition to the slow growth regime; however, the surface coverage in this regime is not significantly different than the copolymer adsorption without added dioxane. Even though a cosolvent may initially enhance the rate of layer growth, it has little effect on the adsorbed amount at longer times due to significant micelle adsorption to the OTS surface in the first place.

Conclusions

We have examined how PtBS-*b*-NaPSS copolymers can initially populate a barren surface in aqueous environments. Two routes were observed: the adsorption of individual chains and the direct adsorption of micelles. Free chain adsorption occurs rapidly and is primarily limited by the supply rate to a strongly attractive surface. Micelles, on the other hand, adsorb more slowly than the associated diffusion rates would suggest. In order for a micelle to adsorb, the corona must deform, an energetically unfavorable event. The rate at which micelles can contribute to the growing layer should then be determined by a balance between the compressibility of the corona and the strength of the micelle−surface interaction. If the strength of the micelle−corona interaction is sufficiently weak, as observed for the hydrophilic SiO_2 surface, micelle adsorption is strongly hindered and growth of the adsorbed layer results overwhelming from free chain adsorption. In situations where a block copolymer has a vanishingly small cmc, adsorption may not occur in a reasonable time frame.

Layer growth can also be impacted by micelle relaxation through the expulsion of free chains in the vicinity of the adsorbing substrate. If the characteristic relaxation time is much longer than the characteristic adsorption time, micelle relaxation will have minimal effect on the adsorption process. In the opposite limit, however, micelle relaxation can dramatically enhance rates of adsorption, at least initially. As the adsorbed layer fills in, diffusion through a partially formed layer eventually limits adsorption, and micelle relaxation becomes less important.

More generally, these findings demonstrate that the adsorption of block copolymers cannot be interpreted without knowledge of the mechanisms of assembly. In the case of very low cmcs, adsorption time scales may extend over weeks, if not years, to approach equilibrium surface coverage. On the other hand, if micelle adsorption is active and contributes significantly to the growth of the adsorbed layer, the structure and homogeneity of the layer may be affected more by the micellar properties than by true equilibrium. In either case, the

effect of micellization must be fully understood in order to properly anticipate the surface coverage achievable within reasonable time frames.

Acknowledgment. The work at UCSB was supported by the NIRT Program and MRL Program of the National Science Foundation under Awards No. CTS-0103516 and DMR-0080034. Work at UT and ORNL was supported by the Division of Chemical Sciences, Geosciences, and Biosciences, Office of Basic Energy Sciences, U. S. Department of Energy, under Contract No. DE-AC05-00OR22725 with Oak Ridge National Laboratory, managed and operated by UT-Battelle, LLC.

References and Notes

(1) Tassin, J. F.; Siemens, R. L.; Tang, W. T.; Hadziioannou, G.; Swalen, J. D.; Smith, B. A. *J. Phys. Chem.* **1989**, *93*, 2106−2111.
(2) Tirrell, M.; Parsonage, E.; Watanabe, H.; Dhoot, S. *Polym. J.* **1991**, *23*, 641−649.
(3) Amiel, C.; Sikka, M.; Schneider, J. W.; Tsao, Y. H.; Tirrell, M.; Mays, J. W. *Macromolecules* **1995**, *28*, 3125−3134.
(4) Motschmann, H.; Stamm, M.; Toprakcioglu, C. *Macromolecules* **1991**, *24*, 3681−3688.
(5) Abraham, T.; Giasson, S.; Gohy, J. F.; Jerome, R.; Muller, B.; Stamm, M. *Macromolecules* **2000**, *33*, 6051−6059.
(6) Styrkas, D. A.; Bütün, V.; Lu, J. R.; Keddie, J. L.; Armes, S. P. *Langmuir* **2000**, *16*, 5980−5986.
(7) De Cupere, V. M.; Gohy, J.-F.; Jerome, R.; Rouxhet, P. G. *J. Colloid Interface Sci.* **2004**, *217*, 60−68.
(8) Hamley, I. W.; Conell, S. D.; Collins, S. *Macromolecules* **2004**, *37*, 5337−5351.
(9) Dan, N.; Tirrell, M. *Macromolecules* **1993**, *26*, 4310−4315.
(10) Johner, A.; Joanny, J. F. *Macromolecules* **1990**, *23*, 5299−5311.
(11) Marques, C.; Joanny, J. F.; Leibler, L. *Macromolecules* **1988**, *21*, 1051−1059.
(12) Munch, M. R.; Gast, A. P. *Macromolecules* **1988**, *21*, 1366−1372.
(13) Schneider, H. M.; Frantz, P.; Granick, S. *Langmuir* **1996**, *12*, 994−996.
(14) Dewalt, L. E.; Ouyang, H. D.; Dimonie, V. L. *J. Appl. Polym. Sci.* **1995**, *58*, 265−269.
(15) Hong, P. P.; Boerio, F. J.; Tirrell, M.; Dhoot, S.; Guenoun, P. *Macromolecules* **1993**, *26*, 3953−3959.
(16) Webber, G. B.; Wanless, E. J.; Armes, S. P.; Baines, F. L.; Biggs, S. *Langmuir* **2001**, *17*, 5551−5561.
(17) Halperin, A.; Joanny, J. F. *J. Phys. II* **1991**, *1*, 623−636.
(18) Bijsterbosch, H. D.; Stuart, M. A. C.; Fleer, G. J. *Macromolecules* **1998**, *31*, 9281−9294.
(19) Munch, M. R.; Gast, A. P. *Macromolecules* **1990**, *23*, 2313−2320.
(20) Israelachvili, J. *Intermolecular and Surface Forces*; Academic Press: New York, 1992.
(21) Munch, M. R.; Gast, A. P. *J. Chem. Soc., Faraday Trans.* **1990**, *86*, 1341−1348.
(22) Valint, P. L.; Bock, J. *Macromolecules* **1988**, *21*, 175−179.
(23) Yang, J.; Mays, J. W. *Macromolecules* **2002**, *35*, 3433−38.
(24) Yang, J. C.; Jablonski, M. J.; Mays, J. W. *Polymer* **2002**, *43*, 5125−5132.
(25) Jasperson, S.; Schnatterly, S. *Rev. Sci. Instrum.* **1969**, *40*, 761.
(26) Azzam, R. M.; Bashara, N. M. *Ellipsometry and Polarized Light*; North-Holland Publication: Amsterdam, 1979.
(27) Toomey, R.; Mays, J.; Tirrell, M. *Macromolecules* **2004**, *37*, 905−911.
(28) Zhang, Y. Y. Ph.D. Thesis, University of Minnesota, 1996.
(29) Dünweg, B.; Reith, D.; Steinhauser, M.; Kremer, K. *J. Chem. Phys.* **2002**, *117*, 914−924.
(30) Kawaguchi, M.; Hayashi, K.; Takahashi, A. *Macromolecules* **1984**, *17*, 2066−2070.
(31) Hesselink, F. T. *J. Colloid Interface Sci.* **1977**, *60*, 448−466.
(32) Yim, H.; Kent, M.; Matheson, A.; Ivkov, R.; Satija, S.; Majewski, J.; Smith, G. S. *Macromolecules* **2000**, *33*, 6126−6133.
(33) Guenoun, P.; Davis, H. T.; Tirrell, M.; Mays, J. W. *Macromolecules* **1996**, *29*, 3965−3969.
(34) Guenoun, P.; Lipsky, S.; Mays, J. W.; Tirrell, M. *Langmuir* **1996**, *12*, 1425−1427.
(35) van Stam, J.; Creutz, S.; De Schryver, F. C.; Jerome, R. *Macromolecules* **2000**, *33*, 6388−6395.

MA048121X